HEDL-SA-824

CONF-760530--6

DEPENDENCE OF IRRADIATION CREEP ON TEMPERATURE AND ATOM DISPLACEMENTS IN 20% COLD WORKED TYPE 316 STAINLESS STEEL

By

E. R. Gilbert

April 1976

For presentation at the International Colloquium on Measurement of Irradiation Enhanced Creep in Nuclear Materials to be held at Petten, Netherlands, May 5-6, 1976.

HANFORD ENGINEERING DEVELOPMENT LABORATORY
Richland, Washington
operated by
WESTINGHOUSE HANFORD COMPANY
a subsidiary of Westinghouse Electric Corporation
for the
UNITED STATES ENERGY RESEARCH AND DEVELOPMENT ADMINISTRATION
UNDER CONTRACT E(45-1)-2170

HEDL-SA-824

DEPENDENCE OF IRRADIATION CREEP ON TEMPERATURE AND ATOM DISPLACEMENTS IN 20% COLD WORKED TYPE 316 STAINLESS STEEL

By

E. R. Gilbert

ABSTRACT

Irradiation creep studies with pressurized tubes of 20% cold worked Type 316 stainless steel were conducted in the Second Experimental Breeder Reactor. These studies have shown that as atom displacements are extended above 5 dpa and temperatures are increased above 375°C, the irradiation induced creep rate increases with both increasing atom displacements and increasing temperature. The stress exponent for irradiation induced creep remained near unity. Irradiation induced effective creep strains up to 1.8% were observed without specimen failure.

INTRODUCTION

Most irradiation creep experiments in fast reactors have been limited to temperatures below 450°C and to atom displacements around 5 to 10 dpa. The results have shown irradiation creep to be linear with stress, atom displacement, and rather insensitive to temperature. Early measurements of irradiation creep in thermal reactors showed similar results for stress and neutron fluence dependence, but Hesketh (1) found the creep rate of nickel to double when the irradiation temperature was decreased from 43 to -195°C.

The present experiment was designed to investigate irradiation creep in the range of 375 to 575°C and atom displacements up to 30 dpa* to determine

*Atom displacements were computed according to the Doran damage function (2).

if the insensitivity to temperature and linearity with respect to atom displacement and stress are still observed.

EXPERIMENTAL DETAILS

The results being reported are from the X-157 experiment which consisted of 2.5 cm long segments of helium pressurized Type 316 stainless steel tubes and the instrumented XX03 (3) and XX05 experiments which contained 6 cm long tubes also pressurized with helium. The tubes for both experiment types were manufactured from Heat V87210 tubing Lot No. N2 and are 20% cold worked Type 316 stainless steel. The specimen design is shown in Fig. 1 and the composition for Heat V87210 is given in Table I. The tubing was found to have a mean grain intercept of 25 microns.

The X-157 specimens were irradiated in short 6 cm long subcapsules as described in Fig. 2. The XX05 specimens were irradiated in an instrumented subassembly similar to the XX03 subassembly described in Ref. 3. The X-157 temperatures are based on heat transfer calculations which are estimated to be accurate to ± 20°C, but depend strongly upon the estimated nuclear heating rate. The XX03 and XX05 temperatures are based on Cr-Al thermocouple measurements and are accurate to within ± 5°C. Specimens from both experiment types were irradiated in static sodium originally containing less than 10 ppm impurities.

The diameters and lengths of the specimens were measured both before and after irradiation. All measurements were accurate to at least 2.5 microns, and most of the diameter measurements were accurate to 0.75 microns.

RESULTS

Since each reactor discharge produced specimens with a particular residence time in the reactor, the data were amenable to isochronal type plots. Isochronal strain-stress curves are shown in Fig. 3. The strain generally appears to be linear with stress. A linear regression analysis was performed to provide the 95% confidence limits on both the slope, $\partial\varepsilon_H/\partial\sigma_H)_{dpa}$ and the stress exponent, $n = \partial \ln \varepsilon_H/\partial \ln \sigma_H)_{dpa}$, for each isochronous curve. The stress exponents are plotted in Fig. 4. The nominal values for the stress exponent center around unity and the 95% confidence limits are generally between 0 and 2 indicating that the stress exponent is less than 2.

The mean values for slopes of the isochronous curves are plotted versus atom displacement in Fig. 5. The results of the XX03, the X-157, and the XX05 experiments appear to form a systematic trend of creep strain with atom displacement and temperature. For temperatures below 500°C the datum points appear to be nearly linear with atom displacements, however, above 500°C the creep rate increases with atom displacements. As the temperature is increased for atom displacements greater than 5 dpa, the creep rate increases with temperature. An equation was generated to follow the nominal creep behavior of the specimens. This equation has features of describing an increasing creep rate with temperature and atom displacement as follows:

$$\varepsilon_H/\sigma_H = \{0.67F+5.8\times10^4 e^{-16000/RT}(F-8.5\mathrm{TANH}\tfrac{F}{8.5})\} \times 10^{-6}\ \mathrm{MPa}^{-1} \qquad (1)$$

where ε_H = midwall hoop strain
σ_H = midwall hoop stress
F = dpa
R = 2
T = °K

DISCUSSION

The results obtained from combining the data of experiments XX03, X-157, and XX05 provide a systematic pattern of behavior for irradiation creep of 20% cold worked Type 316 stainless steel in EBR-II. These results are consistent with low temperature and low atom displacement data (3, 4) which show a linear dependence of irradiation creep on atom displacement and stress. However, due to the expanded temperature and atom displacement range of the X-157 and XX05 experiments, some new trends have been discovered which had not previously been demonstrated. The new trends established are that the creep rate increases with atom displacements above 5 dpa and that the creep rate increases with temperature. Earlier results obtained for nickel in the range below 43°C showed that the creep rate doubled as the temperature was decreased from 43 to -195°C (1). That trend is in the opposite direction as displayed in the range of 375 to 575°C. Data in the intermediate range of 250 to 380°C as summarized by Foster et al. (5) showed little temperature dependence.

The pressurized tubes show little transient irradiation creep. The coefficient for transient irradiation creep, proportional to the strain intercept at zero dpa in Fig. 5, is less than 3×10^{-7} MPa^{-1}. The value for 20% cold worked helical springs is typically 1 to 2×10^{-6} MPa^{-1} (6). This small amount of transient irradiation creep is compatible with the observations of Buckley (7) since the direction for diametral creep is normal to the primary working direction for the tube fabrication.

Although the hyperbolic tangent function in Eq. 1 was used to describe the increase in creep rate with atom displacement observed in the results of this study, there is concern about extrapolating Eq. 1 to atom displacements greater than the 30 dpa of the XX05 experiment. The irradiation induced creep strain observed in the PNL-11 fuel pin cladding (8) suggests that Eq. 1 may underestimate irradiation creep at 50 dpa. Assuming that fission gas pressure is the sole source of stress, the fuel cladding strain is compared with the present results and Eq. 1 in Fig. 6. It is observed that Eq. 1 underestimates the strains observed in the PNL-11 fuel pin cladding. On the other hand, if additional stress sources were important such as fuel-cladding mechanical interactions which were not accounted for, then the larger cladding strains would be expected. As the X-157 experiment is extended to higher neutron fluences, it will be important to determine the dependence of irradiation creep on neutron fluence at the higher atom displacements.

Examination of Fig. 5 shows that the increase in temperature dependence on acceleration of creep rate with atom displacement is much greater for temperatures above 500°C than below 500°C. At temperatures below 500°C the microstructure of the irradiated specimens is characterized by a high concentration of Frank loops (9). However, above 500°C the loops are not observed, and instead, a dislocation network is formed with an increase in dislocation density. It is this network structure which appears to be associated with an increased creep rate with temperature.

The in-reactor creep strains are compared in Fig. 7 with data generated on unirradiated specimens in furnaces. This plot shows that the extent of irradiation enhancement over the thermal creep increases with time. This is consistent with the short time, low dpa datum points at the higher temperatures in Fig. 5 which are above the curves for Eq. 1. These apparently have a greater contribution from thermal creep than the high dpa datum points. It is suggestive in Fig. 7 that irradiation creep, which has previously been limited to low temperature studies, may be important to temperatures as high as 650°C at atom displacements greater than 15 dpa and stresses below 70 MPa.

CONCLUSIONS

1. The irradiation induced creep in 20% cold worked Type 316 stainless steel shows increasing creep rate with increasing temperature and atom displacement in the ranges of 375 to 570°C and 5 to 30 dpa.
2. The dependence of irradiation creep upon stress generally appears to remain linear.
3. Irradiation creep may be important to temperatures as high as 650°C for atom displacements above 15 dpa and stresses below 70 MPa.
4. An effective irradiation induced creep strain of 1.8% was observed in an XX05 specimen without failure.
5. Strains observed in fuel cladding at 50 dpa suggest that the creep rate may increase with atom displacement at a rate faster than accounted for by Eq. 1.

ACKNOWLEDGEMENT

Appreciation is expressed to scientific staff at Westinghouse Hanford Company J. L. Straalsund, J. J. Holmes, and T. T. Claudson for their supporting encouragement and technical guidance.

REFERENCES

1. R. V. Hesketh, "Collapse of Vacancy Cascades to Dislocation Loops," in Proceedings of the International Conference on Solid-State Physics Research with Accelerators, USAEC Report BNL-50083, pp. 389-401, Brookhaven National Laboratory, 1967.
2. D. G. Doran and N. J. Graves, HEDL-TME 73-59, Hanford Engineering Development Laboratory, July 1973.
3. E. R. Gilbert, D. C. Kaulitz, J. J. Holmes and T. T. Claudson, "Fast Reactor Induced Creep in 20% Cold Worked Type 316 Stainless Steel," Proceedings of BNES Conference on Irradiation Embrittlement and Creep in Fuel Cladding and Core Components, p. 239, 1972.

4. D. Mosedale, G. W. Lewthwaite, and I. Ramsay, "Further Creep Experiments in the Dounreay Fast Reactor," Proceedings of BNES Conference on Irradiation Embrittlement and Creep in Fuel Cladding and Core Components, p. 233, 1972.

5. J. P. Foster, W. G. Wolfer, A. Biancheria and A. Boltax, "Analysis of Irradiation-Induced Creep of Stainless Steel in Fast Spectrum Reactors," Proceedings of BNES Conference on Irradiation Embrittlement and Creep in Fuel Cladding and Core Components, p. 273, 1972.

6. D. Mosedale, and G. W. Lewthwaite, "Irradiation Creep in Some Austenitic Stainless Steels, Nimonic PE16 Alloy and Nickel," Proceedings of an Iron and Steel Institute Conference on Creep Strength in Steel and High Temperature Alloys, Sheffield University, 1972.

7. S. N. Buckley, "Irradiation Growth and Irradiation-Enhanced Creep in fcc and bcc Metals," in The Interactions Between Dislocations and Point Defects, proceedings of a symposium held at Harwell, July 4-12, 1968, B. L. Eyre (Ed.), Report AERE-R-5944 (Vol. 2), pp. 547-565, 1968.

8. R. J. Jackson, D. F. Washburn, F. A. Garner, E. R. Gilbert, "Correlation of Creep and Swelling with Fuel Pin Performance," Trans. Am. Nucl. Soc., Vol. 22, p. 184, 1975.

9. H. R. Brager, E. R. Gilbert, and J. L. Straalsund, "The Effect of Stress on the Microstructure of Neutron Irradiated Cold Worked Type 316 Stainless Steel," Radiation Effects, Vol. 21, p. 37, 1974.

TABLE I

CHEMICAL COMPOSITION OF TYPE 316 STAINLESS STEEL

HEAT V87210

Element	Composition, wt. %
Cr	16.5
Ni	13.6
Mo	2.44
Mn	1.63
Si	0.46
C	0.056
N	0.007
P	0.012
S	0.007
Cu	0.07
B	0.0007

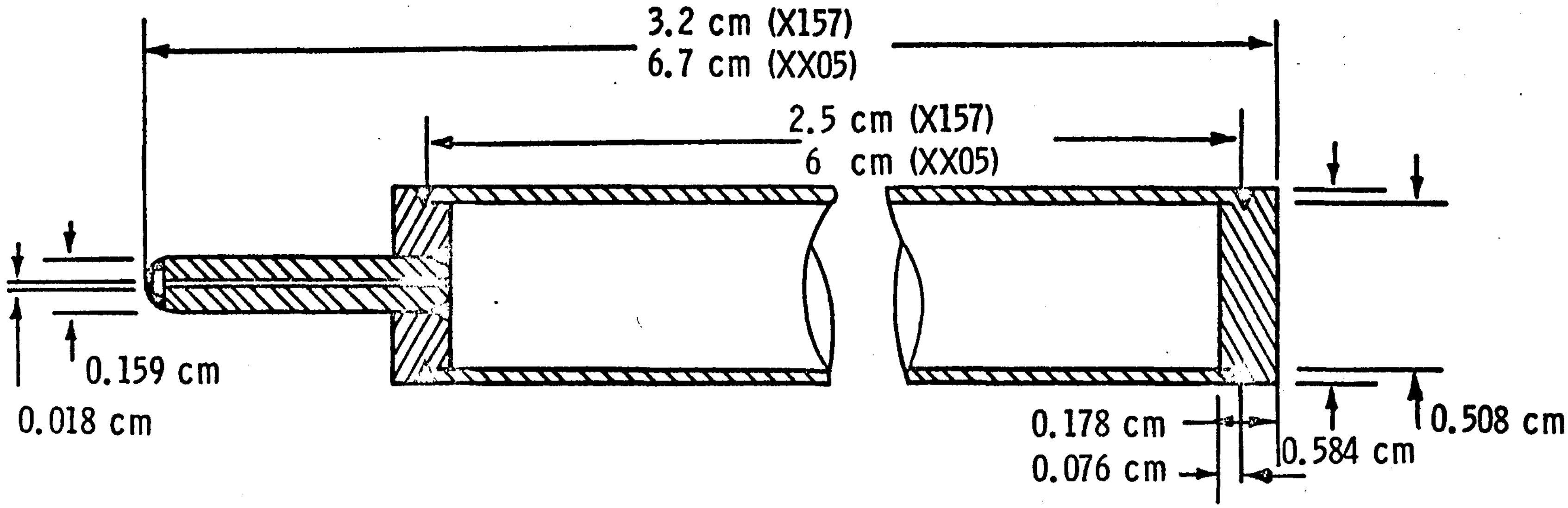

Figure 1. Pressurized Tube Specimen Design.

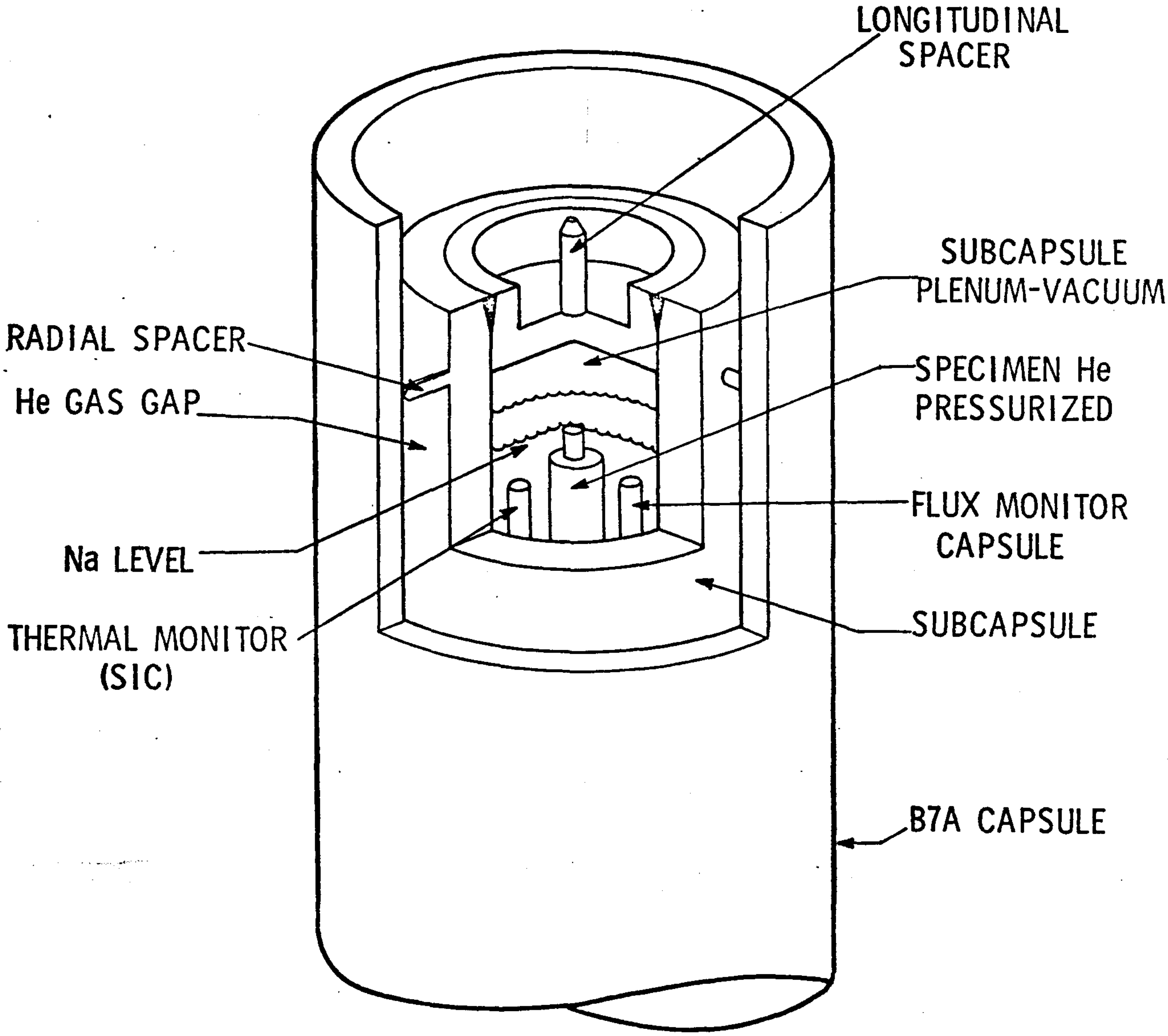

HEDL 7602-116.13

Figure 2. Stressed Cladding Subassembly Arrangement.

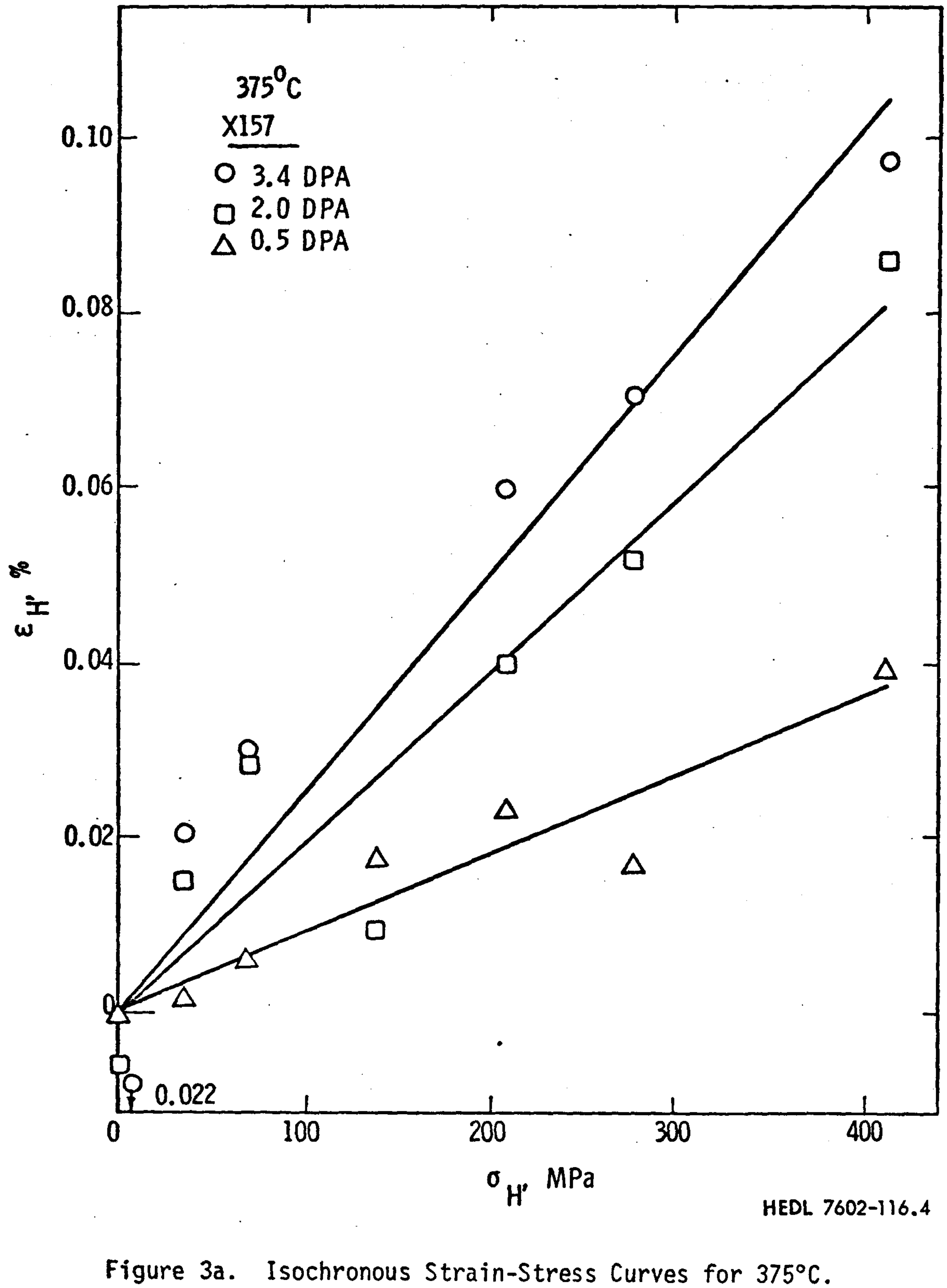

Figure 3a. Isochronous Strain-Stress Curves for 375°C.

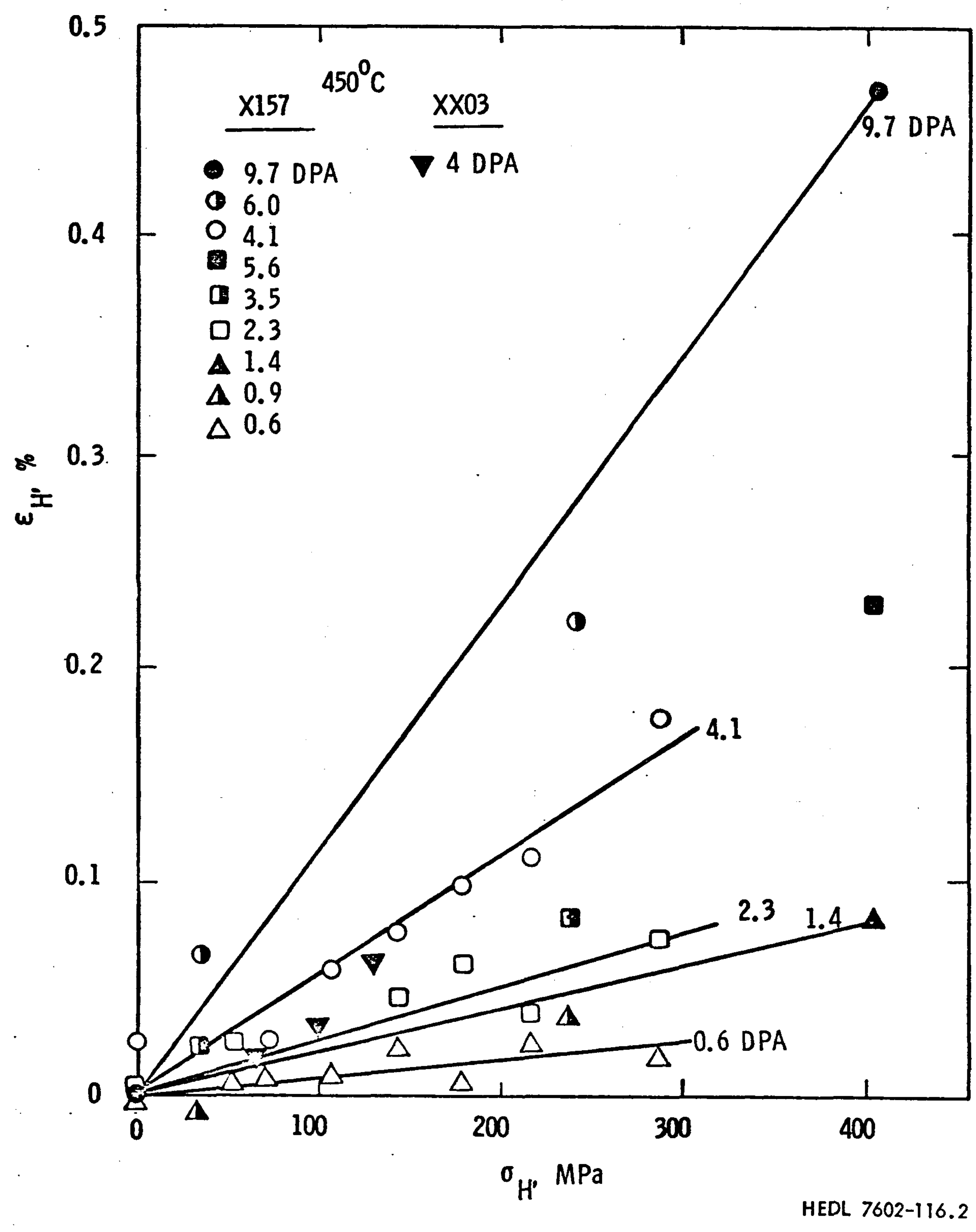

Figure 3b. Isochronous Strain-Stress Curves for 450°C.

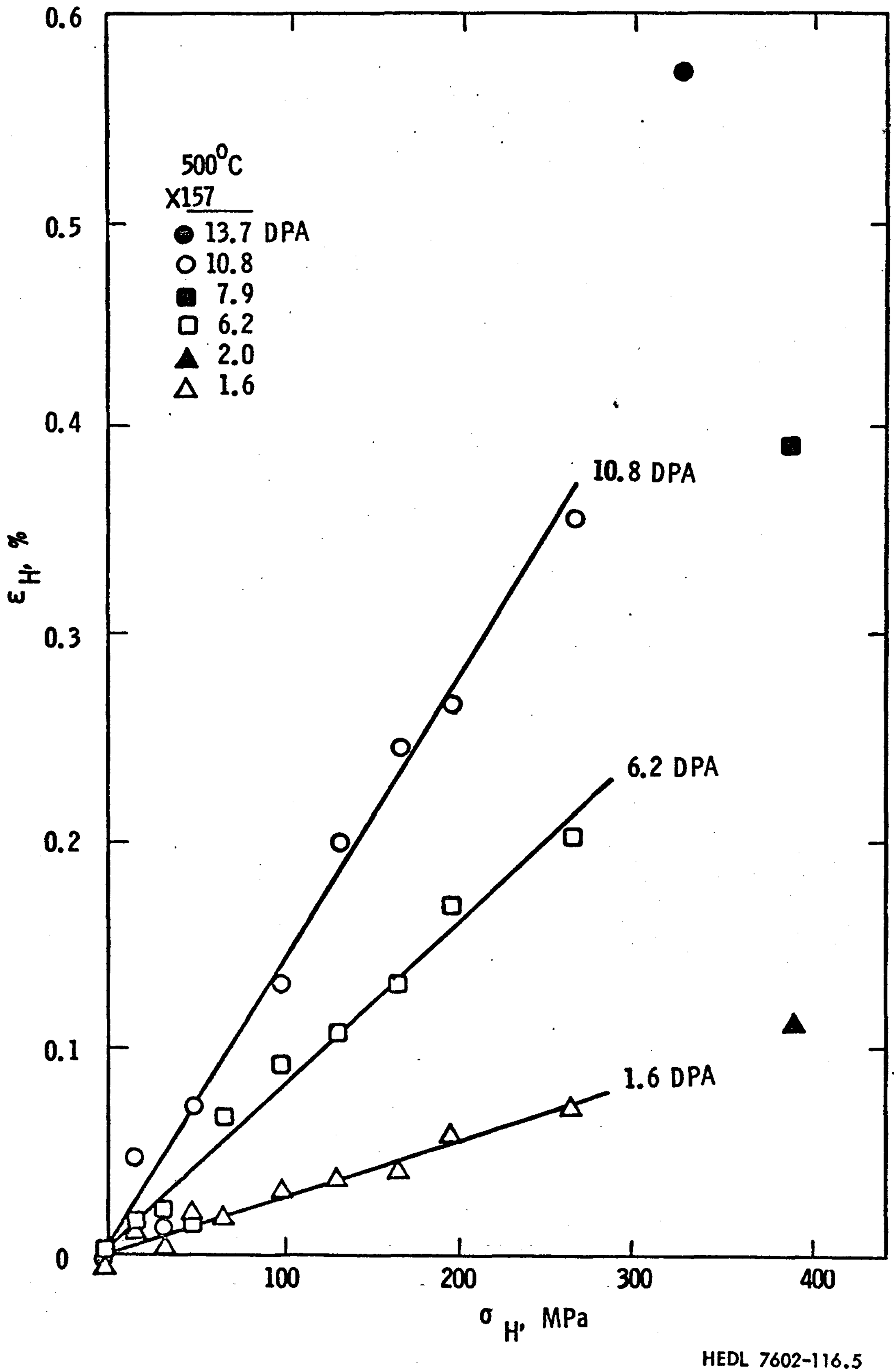

Figure 3c. Isochronous Strain-Stress Curves for 500°C.

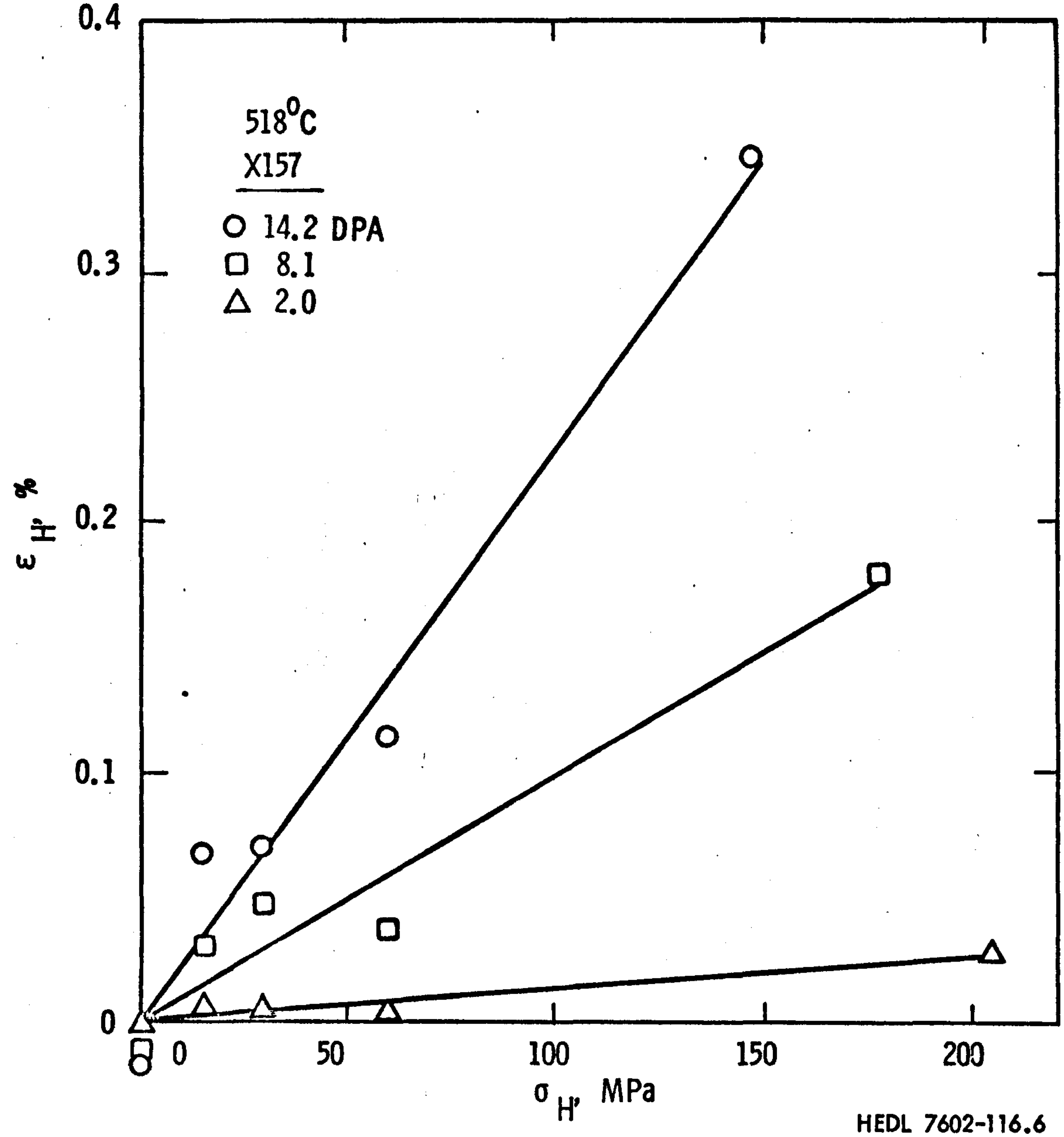

Figure 3d. Isochronous Strain-Stress Curves for 518°C.

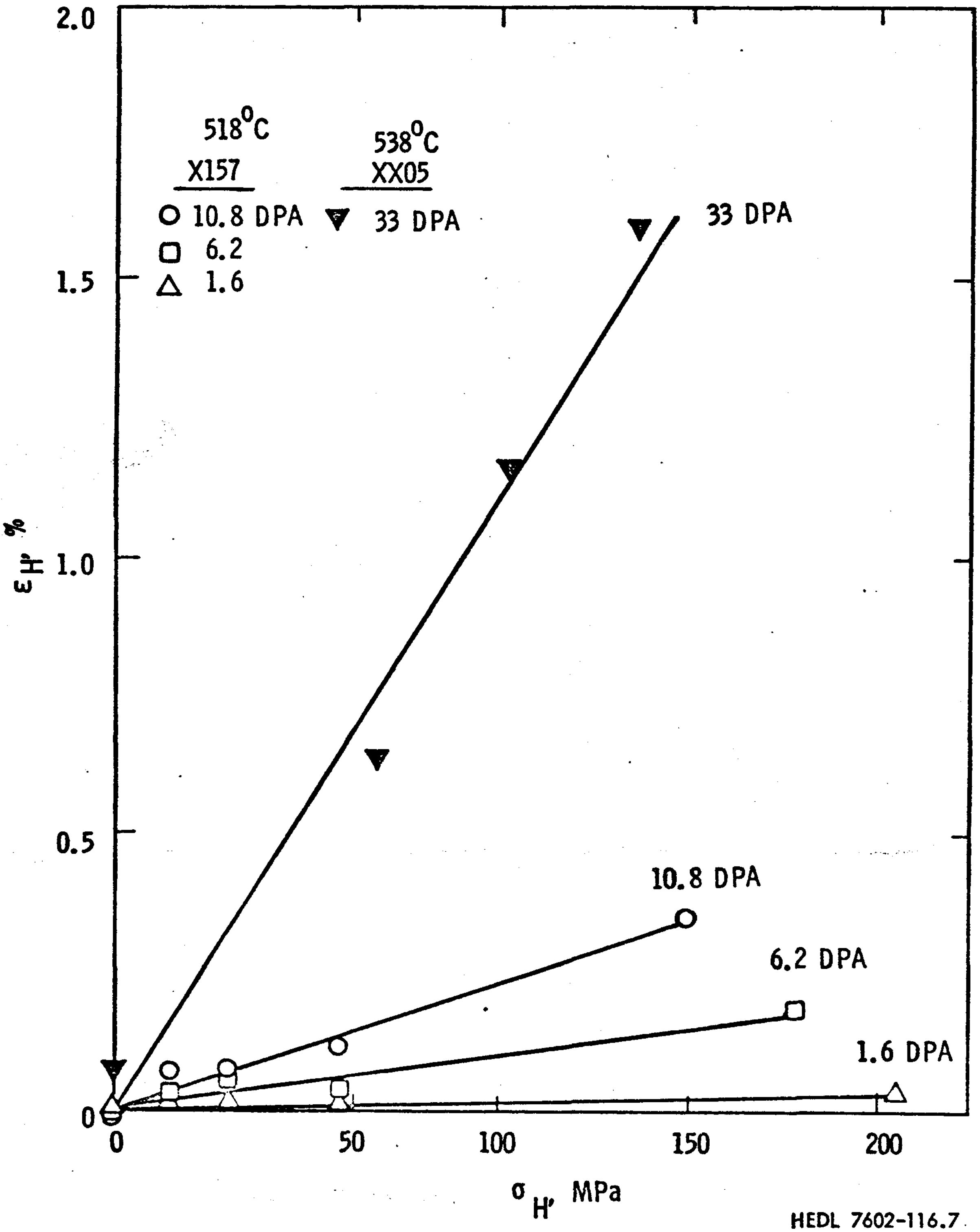

Figure 3e. Isochronous Strain-Stress Curves for 518 and 538°C.

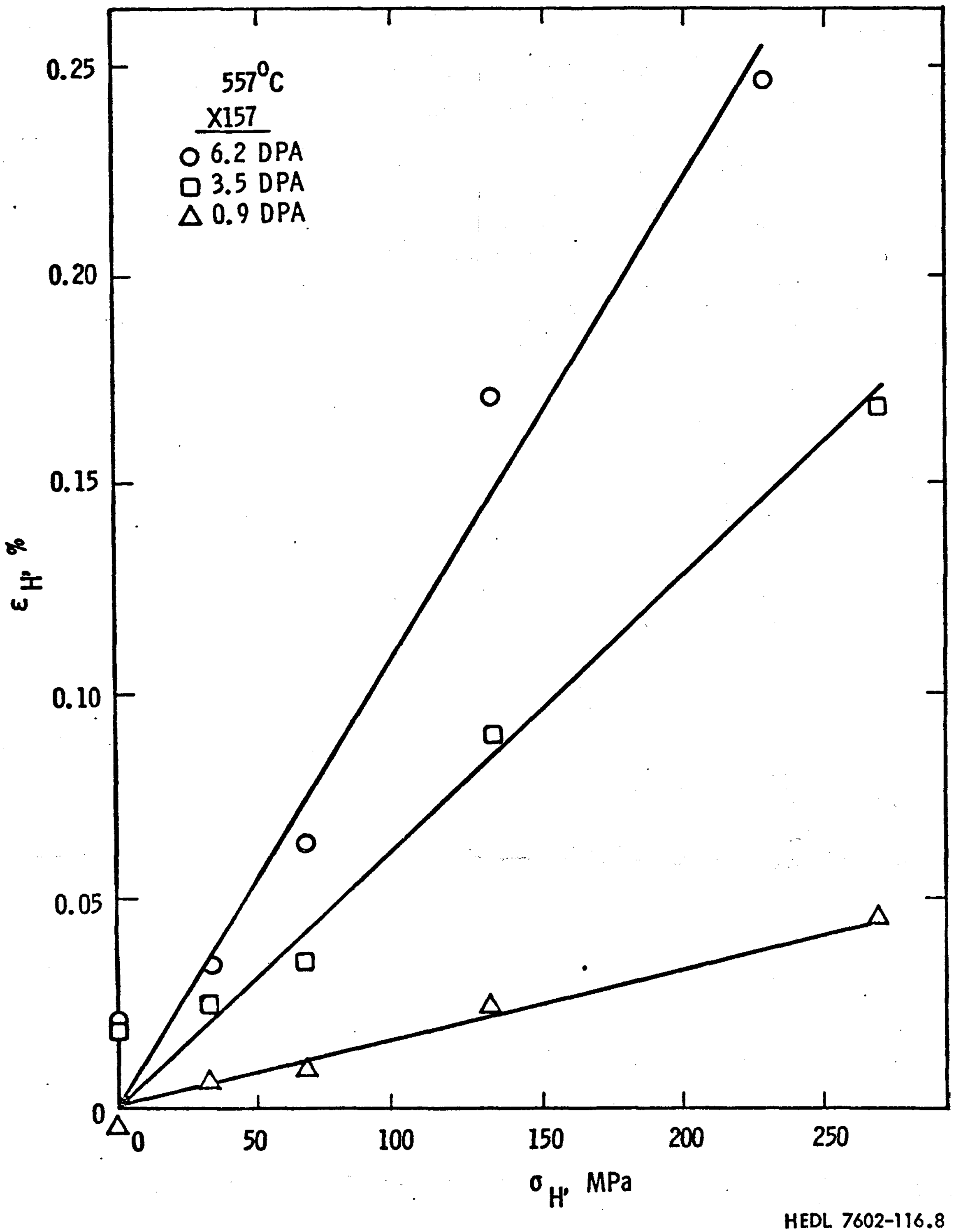

HEDL 7602-116.8

Figure 3f. Isochronous Strain-Stress Curves for 557°C.

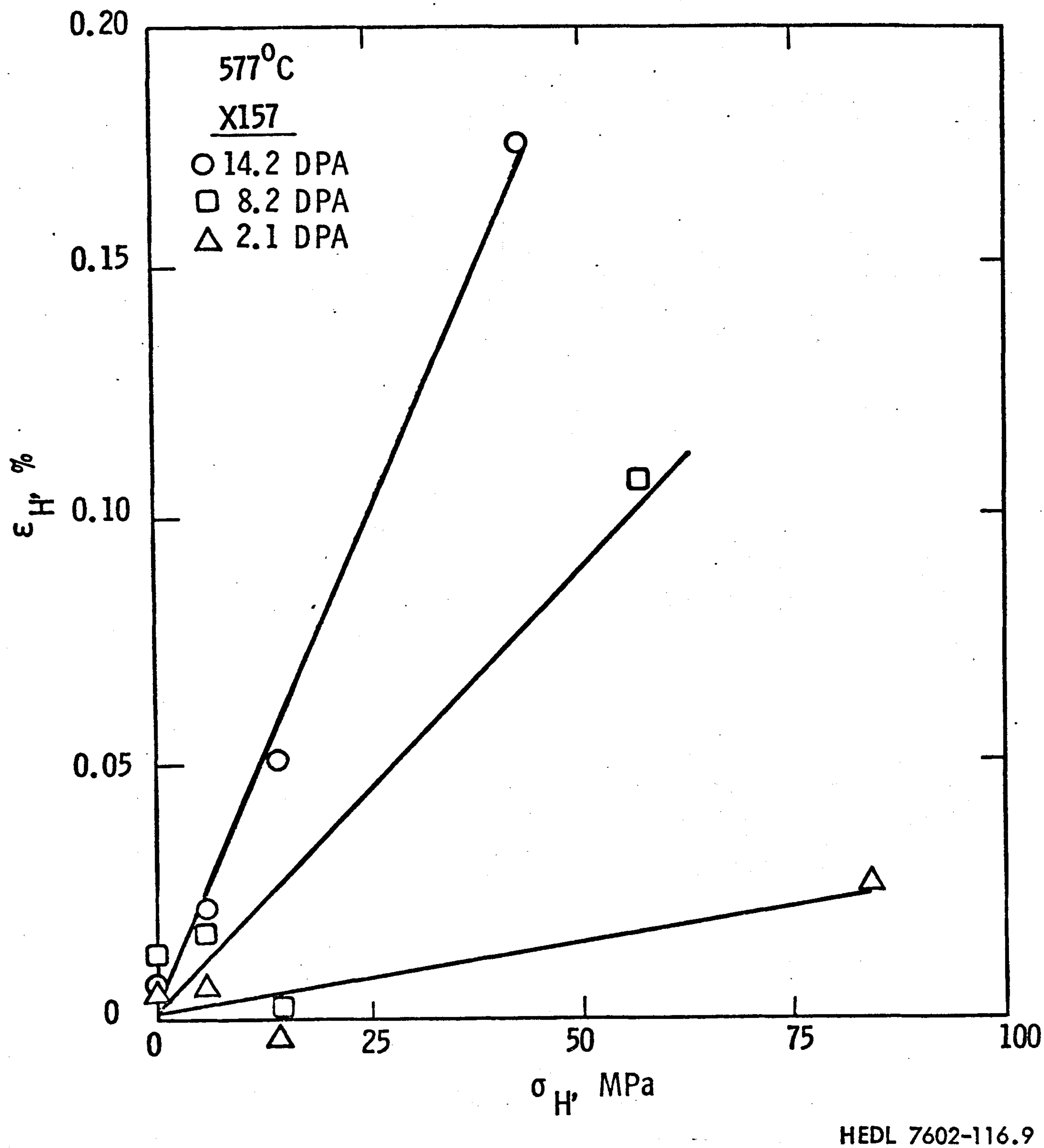

Figure 3g. Isochronous Strain-Stress Curves for 577°C.

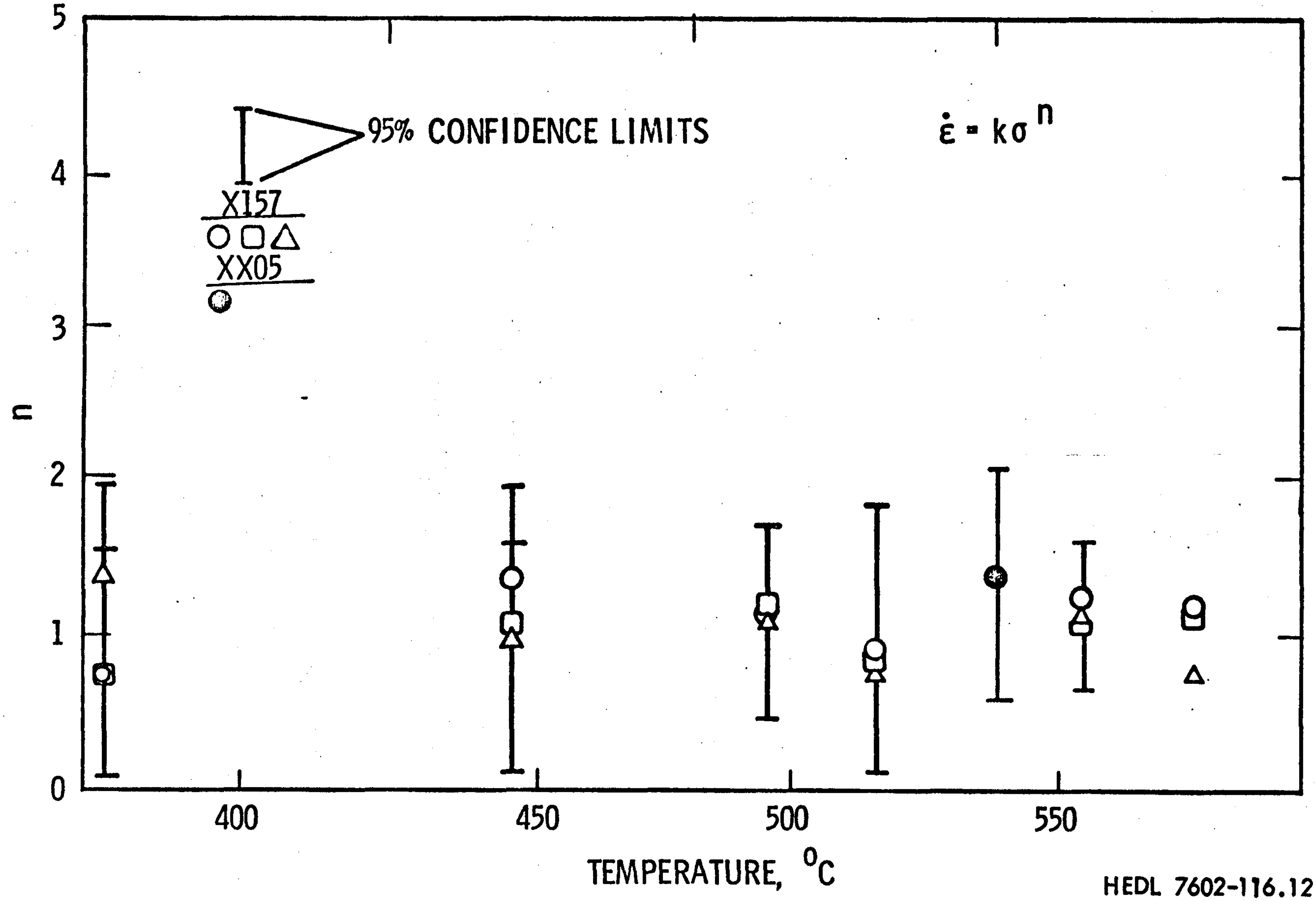

Figure 4. Stress Dependence of Irradiation Creep.

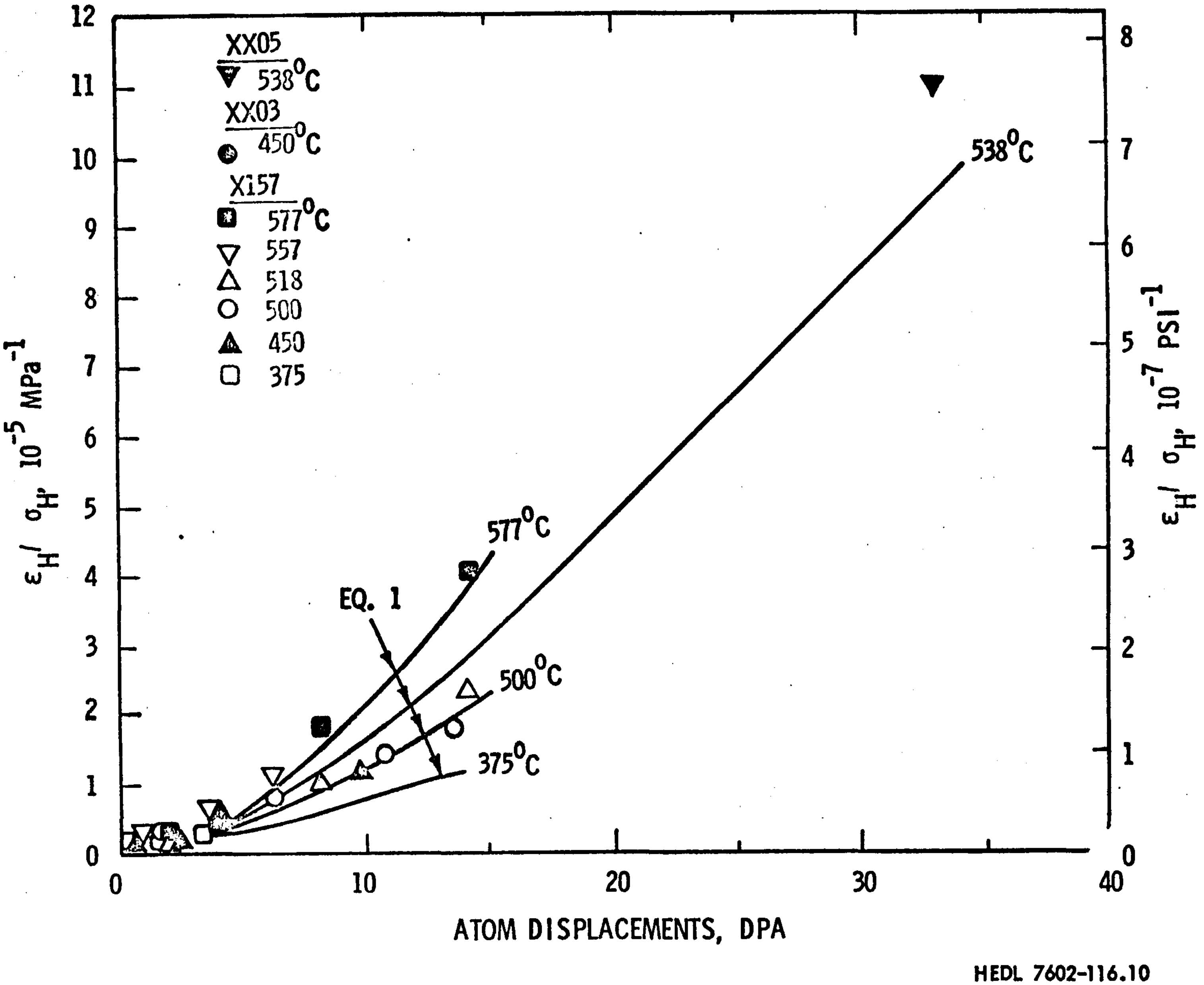

Figure 5. Dependence of Slopes from Isochronous Strain-Stress Curves on Atom Displacements.

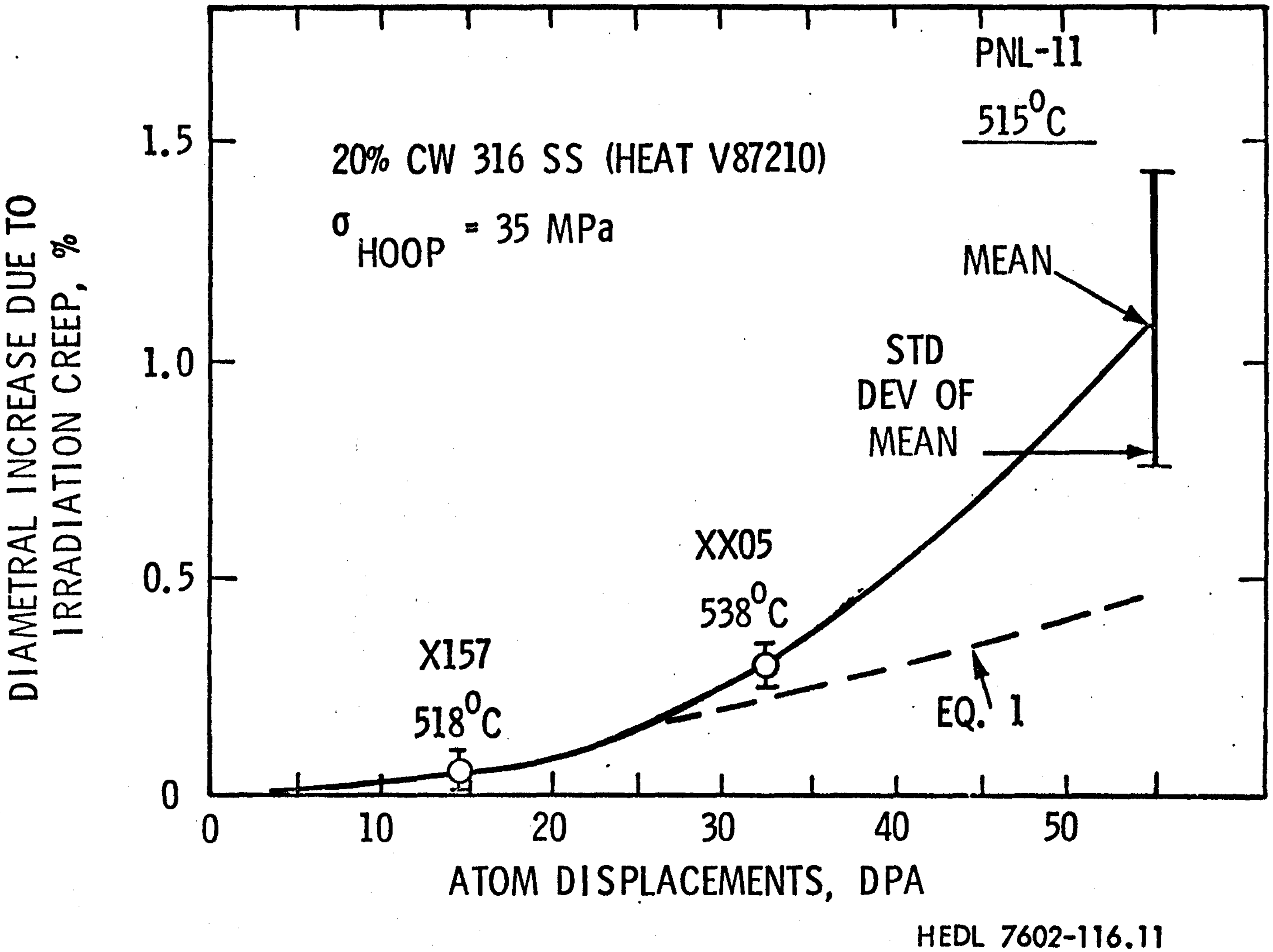

Figure 6. Comparison of Fuel Pin Cladding Strain with Equation 1 and the Results of XX03, X-157, and XX05.

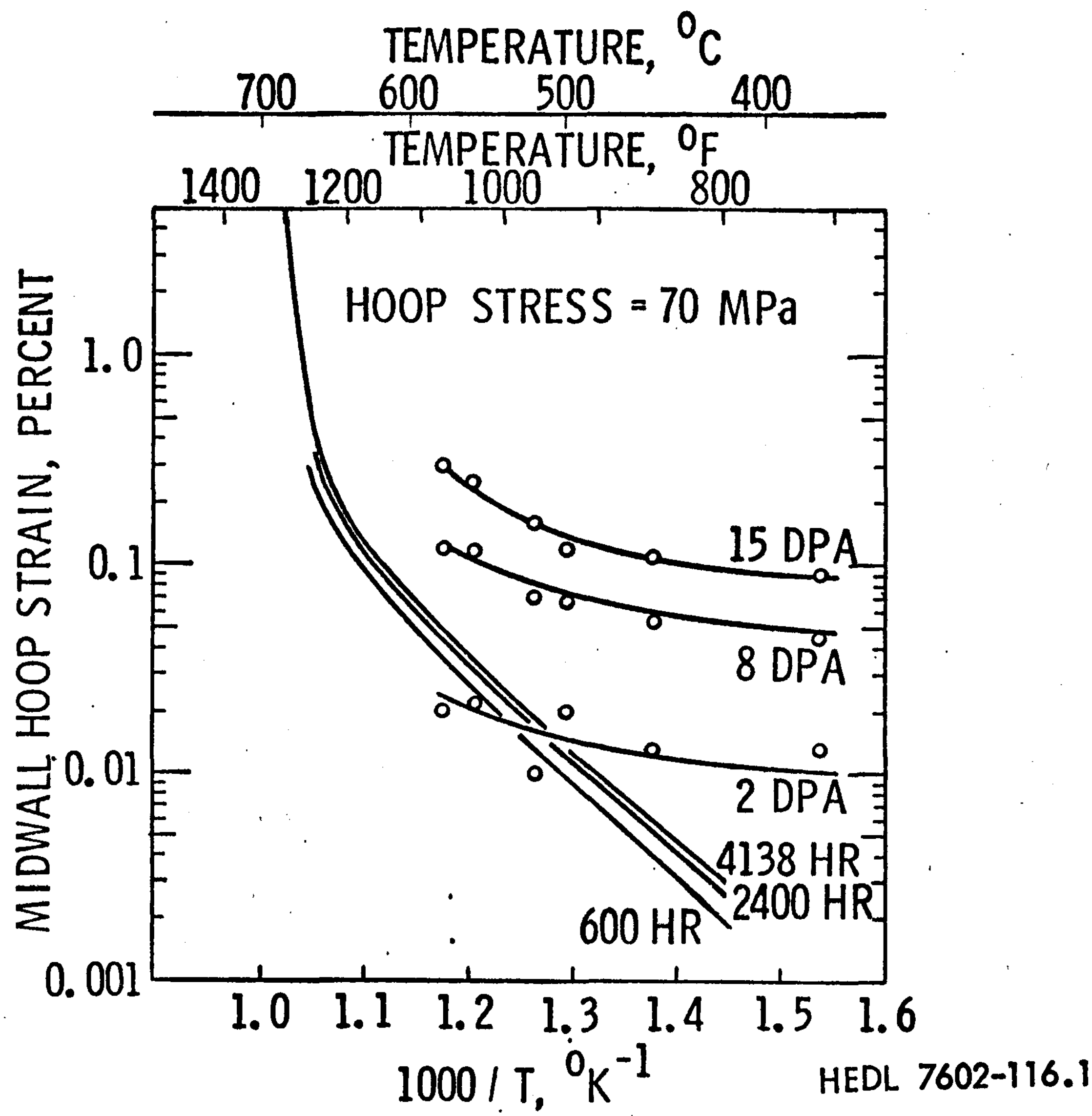

Figure 7. Temperature Dependence of In-Reactor and Thermal Creep for 20% Cold Worked Type 316 Stainless Steel.